analytical chemistry

pubs.acs.org/ac Article

Sensing an Oxygen Sensor: Development and Application of Activity-Based Assays Directly Monitoring HIF Heterodimerization

Liesl K. Janssens and Christophe P. Stove*

Cite This: *Anal. Chem.* 2021, 93, 14462−14470 Read Online

ACCESS | Metrics & More | Article Recommendations | Supporting Information

ABSTRACT: Conventionally, hypoxia-inducible factor (HIF) activation by prolyl hydroxylase domain enzyme (PHD) inhibition is monitored by gene reporter assays. The principle relies on the monitoring of an upstream event (HIF stabilization) by the downstream transcriptional activity. Here, we developed a novel approach to directly sense HIF activation by monitoring the heterodimerization of the HIFα/HIFβ subunits, constituting the functional HIF transcription factor. Two live cell-based biosensor assay setups were designed, utilizing functional complementation of split-nanoluciferase as a tool to measure HIFα/HIFβ protein−protein interaction resulting from the stabilization of HIF1α or HIF2α. The assay setup in a 96-well format was optimized for a duration of 2 h, and a HEK293T transfection protocol was introduced for the optimal configuration of HIFα/HIFβ-fusion proteins. These new bioassays outperformed hypoxia response element-based gene reporter assay, the current state-of-the-art assay, in terms of sensitivity. Applicability was demonstrated using a panel of PHD inhibitors, including roxadustat, molidustat, daprodustat, desidustat, vadadustat, and FG-2216, for which concentration−response curves were generated, allowing for the derivation of potency (EC_{50}) and efficacy (E_{max}) data. The broad applicability of the biosensors was established via applying hypoxia mimetic $CoCl_2$, iron chelator desferrioxamine, proteasome inhibitor MG-132, and 2-OG mimetic dimethyloxalylglycine on the assays, indicating concentration-dependent effects.

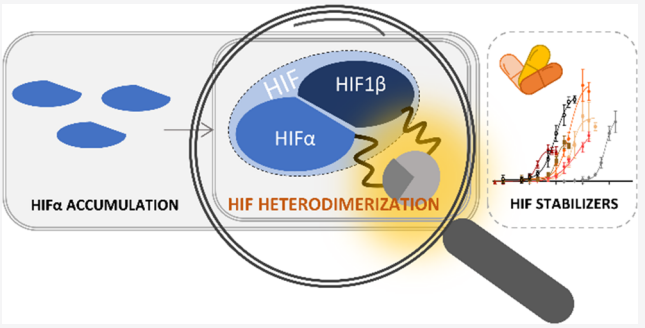

The ability of cells to sense oxygen levels and adapt cellular processes to low oxygen environments is mainly mediated by hypoxia-inducible factors (HIFs). These are heterodimeric transcription factors, consisting of a HIFα and a HIFβ subunit, of which HIFβ is constitutively expressed in the cells. The HIFα levels, however, are highly oxygen-dependent because of post-translational modifications. Under normoxic conditions, the HIFα subunit is actively hydroxylated by HIF prolyl hydroxylase domain enzymes (PHDs), targeting HIFα for interaction with the von Hippel-Lindau tumor suppressor protein (pVHL), yielding a complex that provides HIFα ubiquitinylation and subsequent proteasomal degradation (Figure 1). Upon oxygen deprivation, the action of PHDs is impaired, leading to accumulation of HIFα, its translocation to the nucleus, and heterodimerization with the HIFβ subunit to form the functional HIF transcription factor complex. Following the recruitment of coactivators, the HIF transcriptional activity leads to modulation of the expression of a large panel of responsive genes via hypoxia response elements (HREs) situated in the promoter regions of these genes. The ultimate hypoxic response includes the production of various proteins, including the red blood cell activator erythropoietin (EPO).[1,2]

The two principal isoforms of HIFα (HIF1α and HIF2α) form distinct heterodimers (HIF1 and HIF2) with the principal HIFβ subunit, HIF1β, to induce the expression of different, though sometimes overlapping, HIF target genes.[3−5] HIF2α has a more limited distribution, whereas HIF1α is expressed in nearly all cell types. HIF1 (HIF1α−HIF1β heterodimer) is considered to control the early response to hypoxia, while HIF2 (HIF2α−HIF1β heterodimer) activation occurs rather slowly and is more sustained, for example, during chronic hypoxia.[4,6]

Under normoxic conditions, cellular HIFα has a short half-life (i.e., only approximately 5 min for HIF1α) due to the very efficient degradation process that is initiated by the PHD hydroxylase activity.[7] Therefore, PHD is critical in regulating the HIF pathway and can be considered the key oxygen sensor in the process. Besides oxygen, the PHD activity is dependent on the presence of ferrous iron and the substrate 2-oxoglutarate (2-OG). Chemical analogues of 2-OG (2-OG mimetics) have been developed to inhibit the PHD activity

Received: July 12, 2021
Accepted: October 14, 2021
Published: October 22, 2021

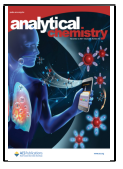

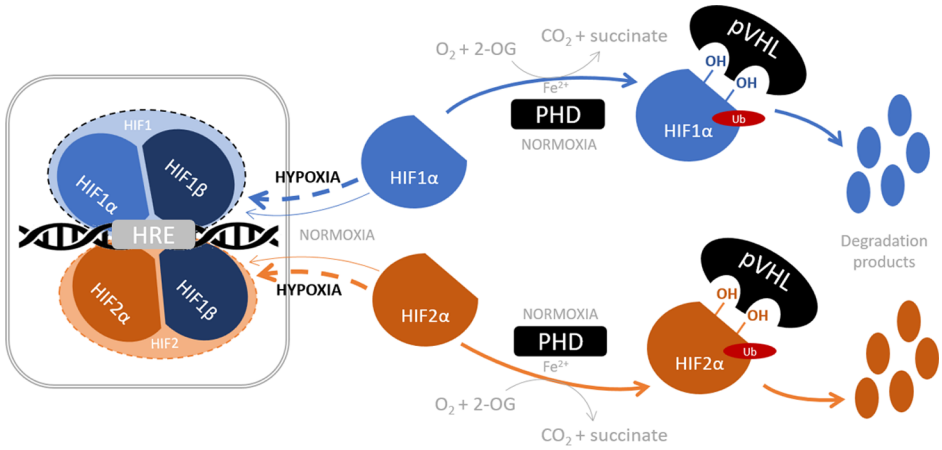

Figure 1. Schematic representation of the HIF signaling pathway. Under normoxia (indicated by full lines), HIFα is targeted for proteasomal degradation through hydroxylation by PHD and ubiquitinylation via interaction with pVHL. Hence, little HIFα is able to translocate to the nucleus. Under hypoxia (indicated by dashed lines), HIF1α/2α is able to accumulate and heterodimerize to an increased extent with HIF1β in the nucleus, forming the functional HIF1/2 transcription factor that binds to HRE sequences in HIF-responsive genes. HIF, hypoxia-inducible factor; HRE, hypoxia response element; PHD, prolyl hydroxylase domain enzyme; pVHL, von Hippel-Lindau tumor suppressor protein; Ub, Ubiquitinyl group; 2-OG, 2-oxoglutarate.

under normoxic conditions, which eventually results in more HIFα/HIFβ heterodimerization and increased HIF-induced transcriptional activation.[5,8] Accordingly, pharmacological approaches to manipulate the HIF pathway by inhibiting the PHD activity have been pursued to treat systemic and local hypoxia-related diseases. As a result, small-molecule xenobiotics (HIF stabilizers) have emerged as a new class of therapeutic drugs to treat anemia.[5,8−11] During drug development and clinical trials, this drug class was also picked up by elite athletes and misused in sports as an alternative for the use of EPO to increase oxygen transport.[12]

HIF stabilizing effects have been characterized at different levels in the HIF signaling pathway, allowing for the derivation of either IC_{50} (monitoring inhibition of PHD enzyme activity) or EC_{50} values (monitoring HIF accumulation or transcriptional activity). PHD inhibition can be measured by mass spectrometry techniques via the detection of reaction products using [^{14}C]-labeled 2-OG or by determining the ratio of parental protein to hydroxylated protein.[7,13,14] Immunoblotting or immunoprecipitation techniques can be used to detect accumulated or hydroxylated HIFα subunits (e.g., hydroxyproline-antibody-based Alpha Screen).[5,10,14] When considering activity-based assays, the traditional gene reporter assays have been the state-of-the-art assays.[5,10,15,16] These assays monitor the level of the HIF transcriptional activity further downstream, using as a read-out the HRE-driven expression of a reporter protein. This read-out is end-point based, relying on the difference in the expression of a reporter gene following HIF activation. A different approach utilizes HIF reporter proteins in which the oxygen degradable domain of the HIFα subunit is fused to luciferase in order to estimate HIFα degradation.[17,18] Both reporter assay types require cell lysis for detection. Other activity-based assays and probes have been developed utilizing fluorescence-based techniques (fluorescence polarization and fluorescence resonance energy transfer) or split-luciferase approaches, monitoring protein−protein interactions within the HIF signaling pathway (HIFα/pVHL and HIFα/HIFβ).[19−25] Contrary to HRE-based gene reporter assays, these "nontraditional" assays have all been employed mainly for research purposes, such as characterizing the heterodimer structure, localizing the HIF subunits, or searching for inhibitors of the HIFα/pVHL or HIFα/HIFβ protein−protein interactions. The existing split-luciferase assay, for example, is specifically designed for characterization of the heterodimerization mechanism and inhibitors thereof and was not applied for (detection of) modulation/regulation of the HIF pathway. Surprisingly, the primary event of HIF activation, that is, HIFα/HIFβ heterodimerization itself, as a mechanism of action, has—to the best of our knowledge—never been used for activity-based detection or characterization of HIF stabilization and HIF modulation. Therefore, we aimed at developing two HIF heterodimerization bioassays based on the two principal isoforms of HIFα to monitor the upstream protein−protein interaction as the result of HIFα accumulation/stabilization in live cells and in real time.

MATERIALS AND METHODS

DMEM, Opti-MEM I Reduced Serum Medium, penicillin/streptomycin (10 000 IU/mL and 10 000μg/mL), amphotericin B (250 μg/mL), glutamine (200 mM), the restriction enzymes *XhoI*, *SalI*, and *SacI*, and DNA polymerase (Phusion polymerase, a polymerase with proofreading activity) were purchased from Thermo Fisher Scientific (Pittsburg, PA, USA). The transfection reagent FuGENE HD and the Nano-Glo Live Cell reagent were purchased from Promega (Madison, WI, USA). Roxadustat was purchased from Toronto Research Chemicals (North York, Canada). Other small-molecule HIF stabilizers (molidustat, daprodustat, FG-2216, vadadustat, and desidustat) and dimethyloxalylglycine (DMOG) were purchased from Cayman Chemical (Ann Arbor, MI, USA). $CoCl_2$, desferrioxamine (DFO), MG-132, custom-synthesized primers, FBS, and poly-D-lysine were procured from Sigma-Aldrich (Steinheim, Germany). The primary antibodies used for immunostaining following western blotting were purchased from Sigma-Aldrich [rat monoclonal anti-HA high affinity and mouse monoclonal Anti-Actin antibody (AC-40)] or Thermo Fisher Scientific [rabbit DYKDDDDK Tag Monoclonal Antibody (FG4R)]. The secondary antibodies were purchased from LI-COR Biosciences—GmbH (Bad Homburg vor der Höhe, Germany;

https://doi.org/10.1021/acs.analchem.1c02923
Anal. Chem. 2021, 93, 14462−14470

IRDye 680RD Goat anti-Rabbit IgG, IRDye 680RD Goat anti-Rat IgG, or IRDye 680RD Goat anti-Mouse IgG).

Molecular Cloning. Plasmids containing the human cDNA for HA-tagged HIFα subunits, HIF1α (NM_001530) and HIF2α (NM_001430), and for FLAG-tagged HIF1β (NM_001668) were purchased from Addgene (Massachusetts, US). Promega provided the plasmids containing the expression vectors (NB MCS-1, NB MCS-2, NB MCS-3, and NB MCS-4), which contain the sequences of the split-NanoLuc luciferase subunits LargeBiT (LgBiT) and SmallBiT (SmBiT) and a flexible serine−glycine linker (GSSGGGGSGGGGSSG). The DNA sequences encoding HA-HIF1α, HA-HIF2α, and FLAG-HIF1β were PCR-amplified with custom-synthesized primers, introducing unique flanking restriction sites (*SacI*, *SalI*, and *XhoI*, respectively) (S1). Fusion constructs were generated by cloning the HIF subunits into the respective NanoBiT expression vectors, generating all possible fusion proteins by standard molecular cloning techniques (HA-HIF1α, HA-HIF2α, and FLAG-HIF1β, either N- or C-terminally fused to SmBiT or LgBiT). The integrity of all constructs was verified by sequencing (Eurofins Genomics LLC, Ebersberg).

Cell Culture. Human embryonic kidney (HEK293T) cells (kindly gifted by Prof. O. De Wever, Laboratory of Experimental Cancer Research, Ghent University Hospital, Belgium) were routinely maintained at 37 °C, 5% CO_2, and under humidified atmosphere and were passaged at 80−90% confluence. They were cultured in DMEM (containing high glucose levels) supplemented with 10% heat-inactivated FBS, 100 IU/mL penicillin, 100 μg/mL streptomycin, and 0.25 μg/mL amphotericin B.

Transient Transfection. A number of 5×10^5 HEK293T cells were seeded into 6-well cell culture plates and incubated overnight to allow for attachment. The next day, the cells were transfected using the FuGENE HD reagent. A constant total amount of DNA [3.3 μg, encompassing plasmids of interest, 100 ng of a plasmid containing enhanced green fluorescent protein (EGFP), complemented with pcDNA3.1] and an optimal ratio of FuGENE/DNA 3:1 were applied. The cells were left to incubate for 6 h before reseeding in the inner wells of white poly-D-lysine coated 96-well microtiter plates (Greiner Bio-one International GmbH, Germany) at a density of 5×10^4 cells/well for subsequent overnight incubation.

Gene Reporter Assay. The HEK293T cells were transfected with 2 μg of the 6xHRE/tk/luc reporter plasmid, kindly provided by P. Ratcliffe and P. Maxwell.[15] The luciferase reporter assay from Promega was performed following the manufacturer's protocol after a 24 h treatment with HIF stabilizers and solvent controls (SCs) in Opti-MEM I Reduced Serum Medium. The outer wells of the 96-well plate were filled with 200 μL of PBS. The assays were performed in a GloMAX96 luminometer (Promega).

Heterodimerization Bioassay. The HEK293T cells, transiently transfected with DNA of expression plasmids encoding a HIFα-fusion protein and a HIF1β-fusion protein (500 ng each), were washed twice with Opti-MEM I Reduced Serum Medium to remove any remaining proteins (present in FBS), and 90 μL of Opti-MEM I was added to each well. Subsequently, the cells were treated with 10 μL of 10× stock solutions or SCs (1% DMSO/Opti-MEM I) to reach the reported in-well concentrations (0.1% DMSO/Opti-MEM I). Stock solutions for higher concentrations of some HIF stabilizers could only be prepared as 1× solutions containing 1% DMSO because their maximal solubility in DMSO was too low in order to dilute down to 0.1% DMSO at the desired concentration of HIF stabilizers (S2). Therefore, the wells encompassing these higher concentrations were directly repleted with 100 μL of 1× stock solutions or SCs after washing the cells. The outer wells were filled with 200 μL of PBS. After 24 h of incubation, fluorescence was measured in a CLARIOstar microplate reader (BMG Labtech, Ortenberg, Germany), and the split-luciferase assay was performed by adding 25 μL of the Nano-Glo Live Cell reagent (Nano-Glo Live Cell substrate diluted 1:20 with Nano-Glo LCS Dilution buffer, Promega) to the wells. This nonlytic detection reagent contains the cell-permeable furimazine substrate. Luminescence was immediately monitored continuously for 2 h in a TriStar^2 LB 942 multimode microplate reader (Berthold Technologies GmbH & Co., Germany) or the CLARIOstar microplate reader for experiments with $CoCl_2$, DFO, and MG-132.

Data Analysis and Statistical Analysis. Data were obtained in a minimum of three independent experiments, and each data point was performed at least in duplicate. The relative luminescence units (RLUs) were used to calculate the area under the curve (AUC) over a period of 2 h as a measure of HIF heterodimerization. All data were evaluated using Grubb's test to detect single outliers. Further data analysis was performed using GraphPad Prism 9 software (San Diego, CA, USA). Potency in terms of HIF heterodimerization (heterodimerization bioassay) or HIF transcriptional activity (gene reporter assay) was determined as EC_{50} values, and efficacy was expressed as E_{max} values by sigmoidal curve fitting the concentration−effect curves via nonlinear regression (four-parametric logistic fit), relative to the PHD inhibitor roxadustat (FG-4592), which was used as a reference (E_{max} values arbitrarily set at 100%). A valid sigmoidal curve fit of this reference was upheld as a prerequisite for acceptance of the data of each independent experiment.

Western Blot Analysis. Total cell lysates (100 μg) of HEK293T cells transfected with one of the three generated fusion constructs (3.3 μg of plasmid DNA) and treated with either 50 μM roxadustat or the SC (1% DMSO/Opti-MEM I) were separated by sodium dodecyl sulfate/PAGE (8.5% acrylamide) at 100 V for 1.5 h and then blotted onto a nitrocellulose membrane. The membrane was incubated for 1 h in blocking buffer [Odyssey blocking buffer (PBS), LI-COR Biosciences—GmbH] at room temperature. Next, the membrane was incubated overnight at 4 °C with the respective primary antibodies and for 1 h at room temperature with the corresponding secondary antibodies, all diluted in the blocking buffer. After each incubation, the membrane was washed three times with PBS supplemented with 0.05% Tween20, followed by a washing step with PBS. The protein signals were detected by a LI-COR Odyssey Infrared Imager (LI-COR Biosciences—GmbH).

RESULTS AND DISCUSSION

Principle and Design of the HIF Assay. The new HIF bioassays were designed utilizing NanoLuc Binary technology (NanoBiT). This technology makes use of a functional complementation-based approach to monitor protein interactions within living cells.[26] By coupling the two inactive subunits of the split-nanoluciferase (NanoLuc), LgBiT (18 kDa) and SmBiT (1 kDa), to the individual subunits of the HIF transcription factor, HIF1α/2α on the one hand and

https://doi.org/10.1021/acs.analchem.1c02923
Anal. Chem. 2021, 93, 14462−14470

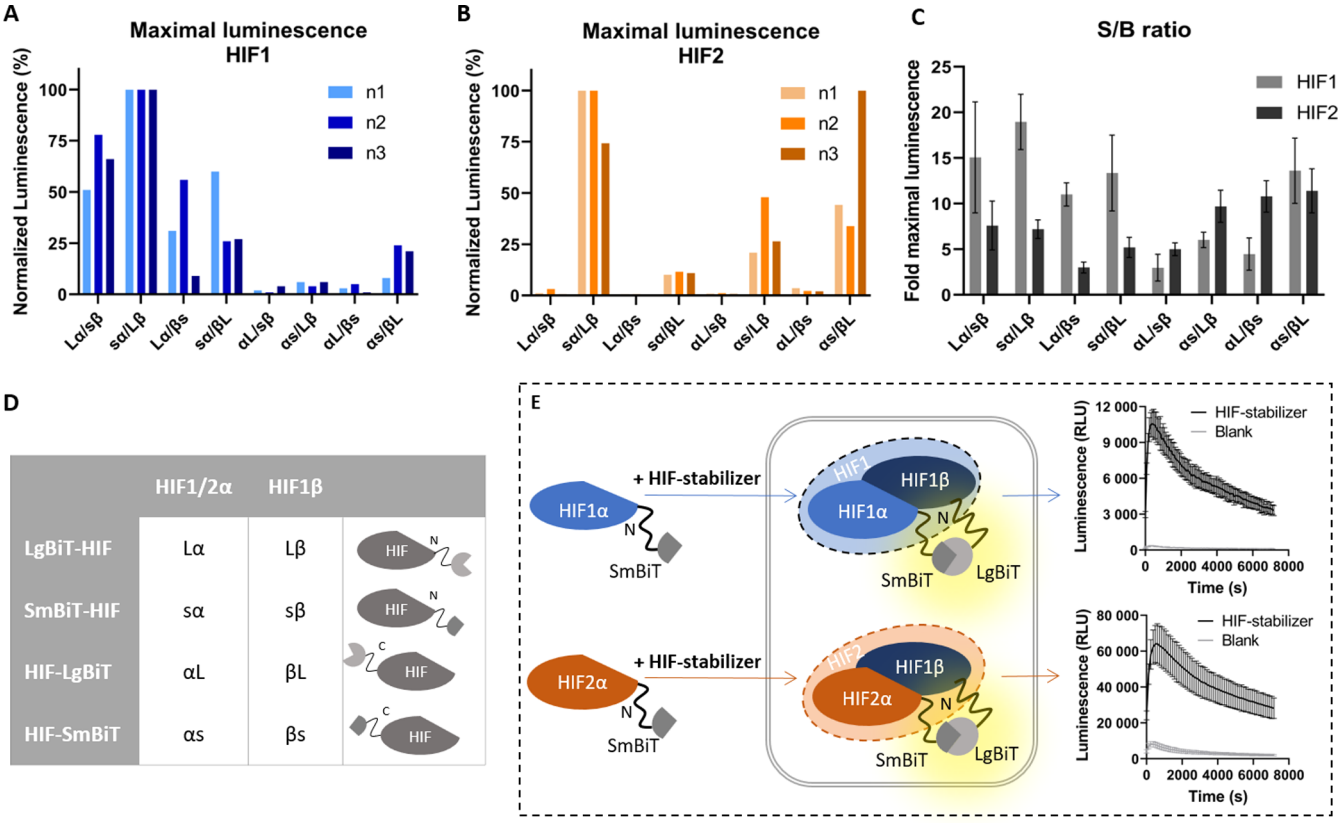

Figure 2. (A,B) Histograms, showing for 3 independent experiments the mean normalized maximal luminescent signals after 24 h treatment with 10 μM roxadustat, comparing the 8 possible configurations of the bioassays for HIF1 (A) and HIF2 (B). (C) Signal over blank (S/B) ratio for the different setups of the HIF1 and HIF2 bioassays (10 μM roxadustat, 24 h). (D) Legend for fusion protein configurations in each tested combination. (E) Principle of the selected HIF bioassays for SmBiT-HIFα/LgBiT-HIF1β, resulting in heterodimerization curves after 24 h treatment with 10 μM roxadustat by monitoring luminescence (RLU ± SEM) in real time as a result of HIF heterodimerization and NanoBiT complementation.

HIF1β on the other, this technology allows for monitoring of the heterodimerization of HIF1 and HIF2 in real time. The *in cellulo* protein−protein interaction of the HIF subunits brings the inactive NanoBiT subunits into close proximity, enabling structural and functional complementation of NanoLuc. The restored luciferase activity results in the production of a measurable bioluminescent signal upon the addition of the furimazine substrate (Figure 2E). The aim of these HIF1 and HIF2 assays is to detect all influences on heterodimerization of the transcription factor, whether degradation or accumulation of HIFα, the latter for example, via stabilization by PHD inhibitors.

To assess functional complementation of the LgBiT- and SmBiT-fusion proteins, we generated all possible configurations and combinations of fusion constructs (the HIF1α/2α subunit on the one hand and the HIF1β subunit on the other, N- or C-terminally fused to SmBiT or LgBiT). In total, this resulted in 16 different combinations (8 for HIF1 and 8 for HIF2), in which we induced stabilization of the HIFα subunit (and thus heterodimerization with HIF1β) using the HIF stabilizer roxadustat (10 μM, 24 h). Regardless of the combination, a baseline bioluminescent signal could be measured when HIFα and HIFβ were both present in the assay.

Moreover, irrespective of the configuration, an increase in the maximal signal could be observed upon HIFα stabilization. In terms of the maximal signal reached in roxadustat-treated cells expressing different combinations, pronounced differences were observed (Figure 2A,B). Overall, the absolute signals were consistently and remarkably higher in the HIF2 bioassay for both SCs and treated cells. To allow for a comparative evaluation, the setup yielding the highest signal was arbitrarily set at 100%, and the signals obtained with the other setups were expressed relative to this maximum (Figure 2A,B). For HIF1, the SmBiT-HIF1α/LgBiT-HIF1β combination consistently yielded the highest signals; this combination also exhibited the highest signal for HIF2 in 2/3 independent experiments (the HIF2α-SmBiT/HIF1β-LgBiT combination yielding the highest signal in one instance). Overall, the lowest signals were observed for those combinations in which HIFα was fused to LgBiT (either C-terminally or N-terminally for HIF2α or only C-terminally for HIF1α) (Figure 2A,B). Also, the extent to which the signal increased upon treatment with 10 μM roxadustat (i.e., signal/baseline ratio; S/B) differed greatly (Figure 2C). For HIF1, the roxadustat treatment resulted in a 3−18-fold increase in luminescence, with a consistent >5- and even >10-fold increase observed for the HIF1α-SmBiT/HIF1β-LgBiT and SmBiT-HIF1α/LgBiT-HIF1β combinations, respectively. For HIF2, a 3−11-fold increased luminescence was observed following the roxadustat treatment, with a consistent >5-fold increase for the SmBiT-HIF2α/LgBiT-HIF1β and HIF2α-SmBiT/HIF1β-LgBiT combinations. Overall, when taking into consideration both the consistently large signal height and a favorable S/B ratio (S3),

https://doi.org/10.1021/acs.analchem.1c02923
Anal. Chem. 2021, 93, 14462−14470

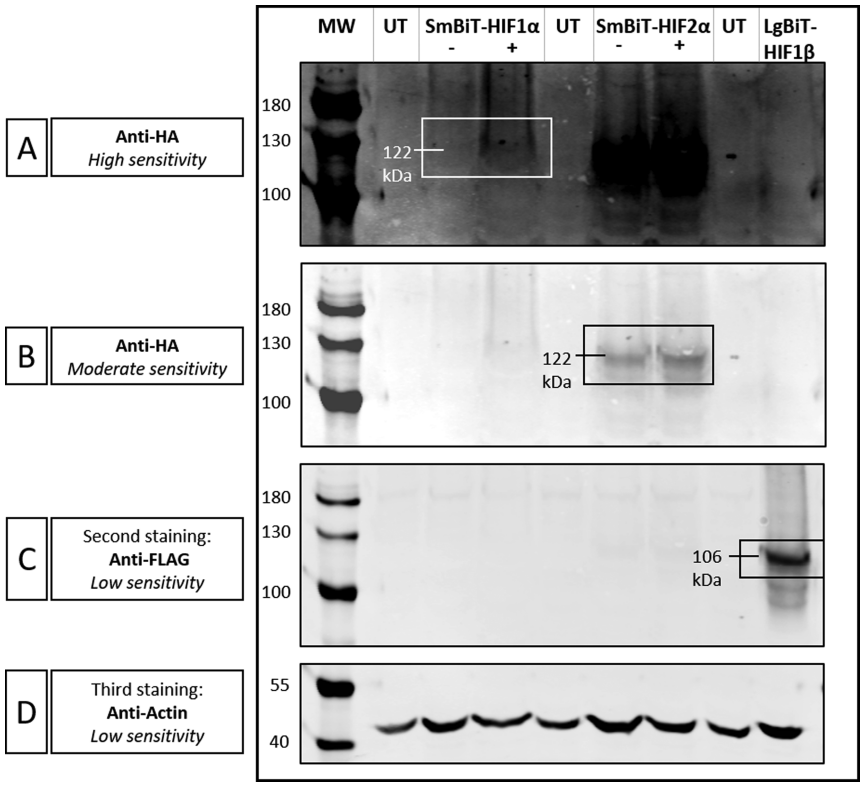

Figure 3. Western blot analysis including three staining procedures (A,B; anti-HA, C; anti-FLAG, and D; anti-Actin) and requiring different instrumental sensitivity based on the level of expression (i.e., high sensitivity for lower expression). MW, molecular weight marker; UT, untransfected HEK293T; −/+, (not) treated with 50 μM roxadustat.

we opted for the SmBiT-HIFα/LgBiT-HIF1β combination to conduct further experiments.

Verification of Protein Expression. Correct expression of the fusion proteins was verified following transient transfection and Western blot analysis, using the incorporated HA- or FLAG-tag for SmBiT-HIFα and LgBiT-HIF1β, respectively (Figure 3). This yielded bands at the expected molecular weights, confirming a higher baseline expression for SmBiT-HIF2α compared to SmBiT-HIF1α (in line with the higher luminescent signals for the HIF2 bioassay) and an increased expression of SmBiT-HIFα upon incubation with roxadustat (50 μM).

Evaluation of Assay Characteristics and Optimization Opportunities. Exploratory experiments made us suspect that the signal obtained in the developed HIF bioassays was related to the positioning of the wells in which the assays were deployed. To further evaluate this, we compared the output from both bioassays, when performed in wells at the outer rim of the 96-well plate versus in wells located more centrally, for SCs and upon 24 h treatment with 10 μM roxadustat. This revealed that the luminescence (AUC) was consistently lower in the inner wells compared to the outer wells for both the HIF1 and HIF2 bioassays, irrespective of whether cells were treated or not (S4). The higher signal in the outer wells is hypothesized to derive from some evaporation of the medium but could also reflect slightly differential oxygen availability, affecting the accumulation of HIFα. Either way, as this adds to the variability of the assay, we only used the inner wells for further testing and repleted the outer wells with 200 μL of PBS at all times to limit the variation stemming from (differential) evaporation.

Further optimization included the evaluation of transfecting alternative amounts of plasmids and differential read-outs. The amount of the transfected plasmid had a considerable effect on the outcome of the assay, primarily because the control situation ("baseline") was greatly influenced. Higher or lower amounts of plasmids used for transfection (respectively 1.6 μg or 200 ng for each plasmid, with the initially used 500 ng as a reference) resulted in higher, respectively lower luminescence signals for both roxadustat-treated and SC-treated cells. Not surprisingly, this indicates that the extent of baseline heterodimerization depends on the amount of protein expressed. Transfection with 500 ng of plasmids turned out to resemble a trade-off between sufficient (induction of) luminescence, while still allowing for enough room for signal increase (S5).

We also evaluated what read-out was best suited to offer an optimal S/B ratio, by comparing the fold signal induction by 10 μM roxadustat, considering the peak signals, as well as the AUC over 30 (AUC30) or 120 min (AUC120). The total run time of the assay was 120 min, taking into account the stability of the substrate to ensure maximal sensitivity. The peak signal was measured between the first 10−20 min of the assay. Therefore, the luminescence measured within the first 30 min has a greater impact on the AUC120, compared to the other 3/4 of the assay duration. A detailed analysis of the output revealed that for both HIF1 and HIF2, the S/B ratio using AUC120 was statistically superior compared to the peak signal and higher compared to AUC30 (S6). Hence, in further experiments, we transfected 500 ng of expression plasmids and used AUC120 as the read-out.

Transfection with a plasmid in which EGFP expression was driven by a cytomegalovirus (CMV) promoter was originally

https://doi.org/10.1021/acs.analchem.1c02923
Anal. Chem. 2021, 93, 14462−14470

included in the transfection protocol to see if it could serve as a means to normalize for experimental variation (inter-well variability). However, the EGFP expression itself was found to be susceptible to the assay conditions that were employed, which could be attributed to the presence of HRE sequences in the CMV promoter (S7). The influence of increased HIF expression on EGFP expression was confirmed experimentally (S7). Therefore, no EGFP-based correction was applied.

Comparison with a State-of-the-Art Activity-Based Bioassay. The performance of the newly developed bioassays was evaluated in comparison to the current state-of-the-art HIF activity-based assay: a traditional HRE-based HIF transcriptional activation assay. This was done by evaluating the assays' sensitivities and by functionally characterizing three HIF stabilizers in all platforms. Sensitivity was appraised by evaluating the ability of the different assay formats to significantly (α = 0.05) distinguish the HIF stabilizing effect of different concentrations of roxadustat from the SC (Figure 4A). The gene reporter assay was capable of detecting the

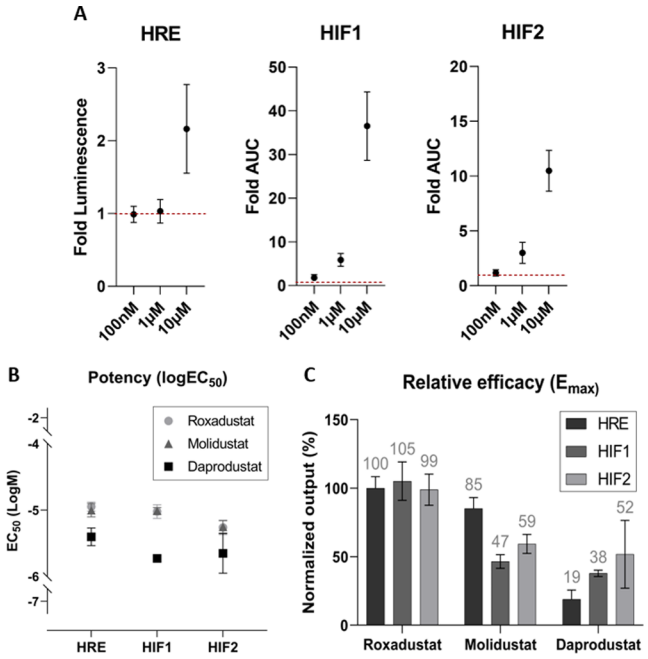

Figure 4. Comparison of the HIF bioassays (HIF1/2) to the state-of-the-art (HRE-based) gene reporter assay. (A) Comparison of sensitivity in terms of the signal/blank (S/B) ratio following 24 h treatment with different concentrations of roxadustat (n = 8). The results are presented as the mean S/B ratio accompanied by the 95CIs. (B) Comparison of potencies, log EC_{50} ± SEM (n = 3), for the indicated PHD inhibitors. (C) Comparison of efficacies, E_{max} ± SEM (n = 3), for the indicated PHD inhibitors, normalized to the E_{max} of roxadustat.

effect of roxadustat at 10 μM, based on the fold induction compared to the blank signal [95%-confidence interval (95CI): 1.55−2.77] but not at 1 μM. Both HIF1/2 heterodimerization assays were found to be more sensitive, readily yielding significantly different signals at a roxadustat concentration of 1 μM (HIF1 95CI: 4.42−7.33 and HIF2 95CI: 2.04−3.96). Furthermore, the HIF1 bioassay could sense roxadustat treatment down to 100 nM (95CI: 1.09−2.50).

Additionally, the performance of the assays was comparatively evaluated by functionally characterizing roxadustat, molidustat, and daprodustat in every platform, deriving potency (EC_{50}—concentration demonstrating 50% activity) and efficacy (E_{max}—maximal activation potential) values as measures for HIF activation. In all three assay formats, roxadustat proved to be the most efficacious, followed by molidustat and daprodustat. The traditional gene reporter assay estimated rather similar HIF transcriptional activity induced by roxadustat and molidustat, both in terms of potency (EC_{50} = 11.3 and 10.0 μM, respectively) and efficacy, while the HIF1/2 bioassays conclude more diverse E_{max} values yet also similar potencies (Figure 4B,C and Table 1). However, only the HIF1 bioassay concluded a significant difference in E_{max} for roxadustat versus molidustat (unpaired t-test, p < 0.05), possibly due to a higher variation of the data in the HIF2 assay. Daprodustat was the most potent in all three assays yet the least efficacious compound. The reported data for the gene reporter assay are in line with the literature, albeit only limited data are available on HIF activation by PHD inhibitors.[5]

In contrast to the current state-of-the-art HRE-based gene reporter assays, the HIF sensors developed here are based on an upstream (heterodimerization) event rather than a downstream (HRE) event. The secondary effects within the cells can interfere with the latter read-out, such as changing protein levels, different cellular behaviors, or cell viability. Assays that score more downstream effects are also more subject to a "plateauing" effect, which poses limitations when assessing efficacy, as discussed elsewhere for other drug targets.[28,29]

Although it is challenging to compare absolute EC_{50} and E_{max} values, the three assays overall yielded concordant results for all compounds tested. Importantly, these data do not reflect PHD inhibition *in se*, where molidustat is estimated to be the most potent PHD inhibitor, followed by roxadustat, with daprodustat estimated to be the least potent.[5,10,14] This observation emphasizes the importance/benefit of HIF activity data (EC_{50}) in HIF research (possibly alongside PHD inhibition data, IC_{50}), as clinical therapy with PHD inhibitors relies on the extent of HIF activation.[10,11,27]

An additional benefit of the HIF bioassays, owing to the assay design, is the possibility to allow for real-time monitoring of the heterodimerization in cells, in contrast to the end-point outcome of the gene reporter assays where cell lysis is required before detection. Moreover, the newly developed assays show promise to perform live measurements in order to reveal time-dependent effects, which have been described in the literature.[5,14] Although in this study, we applied an incubation period with HIF stabilizing conditions before starting the read-out, further research might evaluate whether the assay duration can be lengthened, for example, also allowing for monitoring the onset and/or dynamics of the heterodimerization event. This may be made possible by working in thermostatted conditions while performing the assay and by applying substrates with improved stability (e.g., endurazine).

Application of the HIF Bioassays Using a Panel of HIF Stabilizers. Both HIF1/2 bioassays were applied to generate concentration−response curves for a panel of HIF stabilizers (Figure 5). The overall activity profiles that were obtained, including ranges and ranking orders within each assay, were highly comparable for both HIF1/2 bioassays. EC_{50} and E_{max} values were determined as a measure of relative potency and efficacy, respectively (Table 1). Both assays were able to generate valid four-parametrical fits of sigmoidal curves for all compounds, with the exception of vadadustat, for which no

https://doi.org/10.1021/acs.analchem.1c02923
Anal. Chem. 2021, 93, 14462−14470

Table 1. Potency (EC_{50}) and Efficacy (E_{max}) of a Panel of HIF Stabilizers Determined in the HIF1/2 Bioassays, Accompanied by 95%CIs (n = 3). Roxadustat was Used as a Reference for Relative Efficacy (n = 9)

	HIF1		HIF2	
HIF stabilizer	EC_{50} (μM)	E_{max} (%)	EC_{50} (μM)	E_{max} (%)
roxadustat	9.53 (6.44−28.3)	105 (86.3−182)	5.50 (3.13−14.8)	98.9 (81.8−164)
molidustat	9.77 (7.24−18.3)	46.5 (38.9−75.9)	5.61 (2.62−18.8)	59.4 (47.2−115)
daprodustat	1.86 (1.39−2.65)	37.9 (33.6−45.8)	~2.24[c]	51.8 (>29.3)[d]
vadadustat	[a]	53.5 (45.5−61.4)[b]	~20.0[c]	60.9 (>45.0)[d]
desidustat	32.6 (23.0−127)	119 (100−225)	~22.1[c]	119 (>87.0)[d]
FG-2216	39.1 (20.5−147)	76.0 (59.1−147)	12.1 (5.22−118)	60.8 (48.4−136)
DMOG	693 (530−1489)	77.0 (60.9−141)	495 (>267)[d]	80.0 (>61.4)[d]

[a]No EC_{50} was calculated as no E_{max} was reached. [b]Maximum reached in the assay at 200 μM. [c]Estimation of the parameter without the 95CI. [d]Result accompanied by the lower limit of the incomplete 95CI.

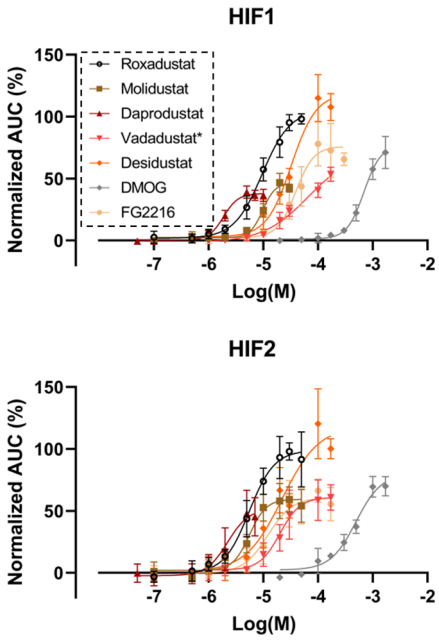

Figure 5. Concentration−response curves for a panel of HIF stabilizers determined in the HIF bioassays. Data are presented as mean ± SEM (n = 3). Roxadustat was used as a reference for normalization (n = 9). *No E_{max} was reached for vadadustat in the HIF1 assay.

maximal HIF1 stabilization was reached at the highest concentration (Figure 5).

All HIF stabilizers—involved in clinical trials/or recently approved on national drug markets—demonstrate more potent HIF stabilization than the 2-OG mimetic, DMOG. Overall, a wide range of EC_{50} values (HIF1: 1.86−693 μM and HIF2: 2.24−495 μM) and E_{max} values (HIF1: 37.9−119% and HIF2: 51.8−119%) was obtained in both heterodimerization assays, indicating an adequate dynamic range. In both HIF1/2 bioassays, daprodustat was the most potent HIF stabilizer (EC_{50} = 1.86 μM/2.24 μM), while desidustat showed the highest efficacy (E_{max} = 119%/119%).

Throughout the entire panel, complete activity profiles were generated in relatively small concentration "windows," with EC_{50} values which were comparable between clusters of compounds [daprodustat < roxadustat ≈ molidustat < FG-2216 ≤ desidustat ≈ vasadustat (only for HIF2) < DMOG]. Efficacy increased in the order of daprodustat, molidustat, (vadadustat) FG-2216, DMOG, roxadustat, and desidustat, with essentially the same rankings obtained for both HIF bioassays.

Although both bioassays could be used for the purpose of compound characterization, as the application of both yielded concentration−response curves, we observed a higher experimental variation for the HIF2 bioassay. This weakens its performance to functionally characterize HIF stabilizing compounds, as demonstrated by larger uncertainties and inconclusive confidence intervals for several PHD inhibitors (Table 1 and Figure 5). It remains to be evaluated whether the generation of stable cell lines (if possible) may help to reduce variability—this is something we are currently exploring.

In general, with the exception of daprodustat, a somewhat lower potency was appraised with the HIF1 bioassay than with the HIF2 bioassay, although the differences were limited and the 95%CIs of the EC_{50} values, if available, were overlapping in all instances. For vadadustat, no EC_{50} could be estimated in the HIF1 bioassay, as no E_{max} was reached at the highest tested concentration (200 μM), in contrast to the HIF2 bioassay, where E_{max} was reached. Also visual interpretation of the activity profiles indicates a greater difference between HIF1α and HIF2α stabilization for vadadustat, compared to all other compounds (S8). Interestingly, to date, vadadustat is the only compound that has been suggested to show α-isoform-selectivity, with a preference toward HIF2α stabilization.[5,30]

Application of the HIF Bioassays is Not Limited to the Evaluation of Clinical PHD Inhibitors. Lastly, to demonstrate the broader applicability of both bioassays, we used these to assess the impact of two hypoxia mimetic treatments often used in hypoxia-related research ($CoCl_2$ and DFO) and a general proteasome inhibitor (MG-132). These compounds induce a hypoxic response by replacing (i.e., $CoCl_2$) or chelating (i.e., DFO) iron, thereby inhibiting the PHD activity indirectly, and via direct inhibition of the proteasomal degradation of HIFα regardless of its hydroxylation status (i.e., MG-132). Figure 6 shows that treatment with all compounds results in a concentration-dependent increase in luminescence within both bioassays (results are represented as mean AUC normalized to the E_{max} of roxadustat). The effects of the compounds in the HIF1 and HIF2 assays are comparable, with the exception of DMOG resulting in more HIF2 stabilization at the applied concentrations, the latter being in line with the generated activity profiles shown in Figure 5.

All the results mentioned above demonstrate that the HIF1 and HIF2 bioassays are general sensors of HIF1α/2α stabilization via the detection of HIF1/2 heterodimerization, regardless of the HIF stabilizing mechanism, whether via 2-OG

https://doi.org/10.1021/acs.analchem.1c02923
Anal. Chem. 2021, 93, 14462−14470

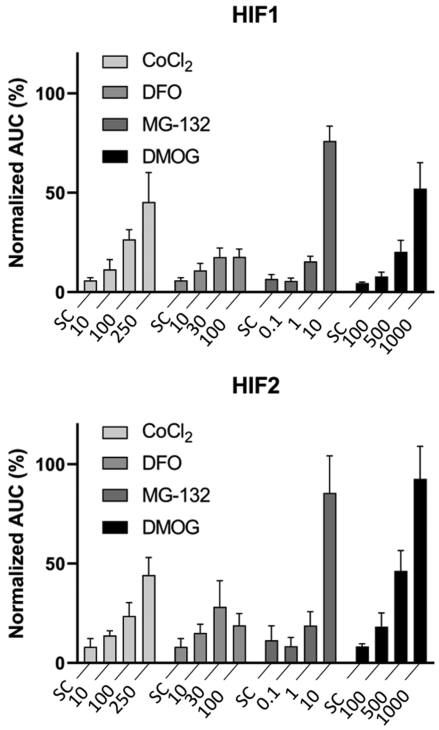

Figure 6. Cumulative luminescent signal (AUC) within the HIF1/2 bioassay after incubation with different concentrations (μM) of $CoCl_2$, DFO, MG-132, and DMOG in comparison to the SC. The results are represented as mean AUC ± SEM, normalized to the E_{max} of roxadustat within three independent experiments.

mimetics (DMOG), direct inhibition of PHD (clinical HIF stabilizers), indirect inhibition of PHD (chelating/replacing iron, necessary for PHD activity), proteasome inhibition, and so forth.

CONCLUSIONS

Two separate activity-based bioassays, capable of monitoring heterodimerization of the two main HIF transcription factors (HIF1/2), were developed in order to sense and study upstream influences on the HIF signaling pathway. These bioassays allow for live and real-time monitoring, with the opportunity to study α-isoform-specific HIF accumulation/stabilization/heterodimerization. These two similarly designed HIF1/2 sensors might prove useful in a variety of contexts. For example, in cancer research, isoform-selective inhibitors of HIF activity are desired, as one isoform may be beneficial, while the other causes harm (e.g., for renal cell carcinoma, it was reported that HIF1α might retard tumor growth, while HIF2α might have an enhancing effect). For such application of the bioassay, it is useful to study both (HIF1/2) heterodimerization processes in parallel to gain fundamental insights regarding, for example, pharmacological features of cancer treatments. Our assay panel might also allow for evaluation of dynamics within the HIF signaling pathway (e.g., onset of HIFα stabilization, duration of stabilization, etc.). Another example of a context where the bioassay can prove useful is doping control, where authorities struggle with the emergence of HIF stabilizers among elite athletes. Here, the most sensitive bioassay (at this moment, the HIF1 bioassay) can prove useful for untargeted screening of athlete samples for HIF stabilizing drugs if the sensitivity is sufficient for the concentrations present in human blood or urine. Also, the transfer of the current transient transfection format to a stable cell line format may prove beneficial in this context. This will be the subject of further research.[5,12,14,24,31,32] Both heterodimerization assays outperformed the state-of-the-art gene reporter assay in terms of sensitivity. The HIF1 bioassay was the most sensitive and would at this point be preferred for general compound characterization as its performance in the current setup seems more robust compared to that of the HIF2 bioassay. In conclusion, these newly developed HIF bioassays may serve as promising platforms for different purposes in further HIF-related research.

ASSOCIATED CONTENT

Supporting Information

The Supporting Information is available free of charge at https://pubs.acs.org/doi/10.1021/acs.analchem.1c02923.

Additional experimental details, methods and results, and other representations of the data (PDF)

AUTHOR INFORMATION

Corresponding Author

Christophe P. Stove − *Laboratory of Toxicology, Department of Bioanalysis, Faculty of Pharmaceutical Sciences, Ghent University, 9000 Ghent, Belgium;* orcid.org/0000-0001-7126-348X; Email: christophe.stove@ugent.be

Author

Liesl K. Janssens − *Laboratory of Toxicology, Department of Bioanalysis, Faculty of Pharmaceutical Sciences, Ghent University, 9000 Ghent, Belgium*

Complete contact information is available at: https://pubs.acs.org/10.1021/acs.analchem.1c02923

Author Contributions

The manuscript was written through the contributions of all authors.

Funding

The authors acknowledge the Bijzonder Onderzoeksfonds (BOF) of Ghent University for granting a doctoral scholarship to L. Janssens (BOF20/DOC/051). The authors also acknowledge financial support from the Partnership for Clean Competition (PCC).

Notes

The authors declare no competing financial interest.

ACKNOWLEDGMENTS

Prof. Peter Van Eenoo is acknowledged by the authors for the joint initiative for this research. The authors acknowledge Prof. O. De Wever for providing HEK293T cells and Promega for providing the NanoBiT expression vectors.

ABBREVIATIONS

AUC	area under the curve
DMOG	dimethyloxalylglycine
DFO	desferrioxamine
FBS	fetal bovine serum
HIF	hypoxia-inducible factor
HRE	hypoxia response element
LgBiT	LargeBiT
PBS	phosphate-buffered saline
PHD	prolyl hydroxylase domain enzyme

pVHL	von Hippel-Lindau tumor suppressor protein
SEM	standard error of means
SmBiT	SmallBit
UT	untransfected
2-OG	2-oxoglutarate
95CI	95%-confidence interval

REFERENCES

(1) Semenza, G. L. *Cell* **2012**, *148*, 399−408.
(2) Wang, G. L.; Jiang, B. H.; Rue, E. A.; Semenza, G. L. *Proc. Natl. Acad. Sci. U.S.A.* **1995**, *92*, 5510−5514.
(3) Dengler, V. L.; Galbraith, M. D.; Espinosa, J. M. *Crit. Rev. Biochem. Mol. Biol.* **2014**, *49*, 1−15.
(4) Stiehl, D. P.; Bordoli, M. R.; Abreu-Rodríguez, I.; Wollenick, K.; Schraml, P.; Gradin, K.; Poellinger, L.; Kristiansen, G.; Wenger, R. H. *Oncogene* **2012**, *31*, 2283−2297.
(5) Yeh, T.-L.; Leissing, T. M.; Abboud, M. I.; Thinnes, C. C.; Atasoylu, O.; Holt-Martyn, J. P.; Zhang, D.; Tumber, A.; Lippl, K.; Lohans, C. T.; Leung, I. K. H.; Morcrette, H.; Clifton, I. J.; Claridge, T. D. W.; Kawamura, A.; Flashman, E.; Lu, X.; Ratcliffe, P. J.; Chowdhury, R.; Pugh, C. W.; Schofield, C. J. *Chem. Sci.* **2017**, *8*, 7651−7668.
(6) Holmquist-Mengelbier, L.; Fredlund, E.; Löfstedt, T.; Noguera, R.; Navarro, S.; Nilsson, H.; Pietras, A.; Vallon-Christersson, J.; Borg, Å.; Gradin, K.; Poellinger, L.; Påhlman, S. *Cancer Cell* **2006**, *10*, 413−423.
(7) Barrett, T. D.; Palomino, H. L.; Brondstetter, T. I.; Kanelakis, K. C.; Wu, X.; Haug, P. V.; Yan, W.; Young, A.; Hua, H.; Hart, J. C.; Tran, D.-T.; Venkatesan, H.; Rosen, M. D.; Peltier, H. M.; Sepassi, K.; Rizzolio, M. C.; Bembenek, S. D.; Mirzadegan, T.; Rabinowitz, M. H.; Shankley, N. P. *Mol. Pharmacol.* **2011**, *79*, 910−920.
(8) Joharapurkar, A. A.; Pandya, V. B.; Patel, V. J.; Desai, R. C.; Jain, M. R. *J. Med. Chem.* **2018**, *61*, 6964−6982.
(9) Pergola, P. E.; Spinowitz, B. S.; Hartman, C. S.; Maroni, B. J.; Haase, V. H. *Kidney Int.* **2016**, *90*, 1115−1122.
(10) Flamme, I.; Oehme, F.; Ellinghaus, P.; Jeske, M.; Keldenich, J.; Thuss, U. *PLoS One* **2014**, *9*, No. e111838.
(11) Besarab, A.; Chernyavskaya, E.; Motylev, I.; Shutov, E.; Kumbar, L. M.; Gurevich, K.; Chan, D. T. M.; Leong, R.; Poole, L.; Zhong, M.; Saikali, K. G.; Franco, M.; Hemmerich, S.; Yu, K.-H. P.; Neff, T. B. *J. Am. Soc. Nephrol.* **2016**, *27*, 1225−1233.
(12) Buisson, C.; Marchand, A.; Bailloux, I.; Lahaussois, A.; Martin, L.; Molina, A. *J. Pharm. Biomed. Anal.* **2016**, *121*, 181−187.
(13) Flagg, S. C.; Martin, C. B.; Taabazuing, C. Y.; Holmes, B. E.; Knapp, M. J. *J. Inorg. Biochem.* **2012**, *113*, 25−30.
(14) Sanghani, N. S.; Haase, V. H. *Adv. Chron. Kidney Dis.* **2019**, *26*, 253−266.
(15) Vaux, E. C.; Wood, S. M.; Cockman, M. E.; Nicholls, L. G.; Yeates, K. M.; Pugh, C. W.; Maxwell, P. H.; Ratcliffe, P. J. *J. Biol. Chem.* **2001**, *276*, 44323−44330.
(16) Miwa, Y.; Hoshino, Y.; Shoda, C.; Jiang, X.; Tsubota, K.; Kurihara, T. *Neurochem. Int.* **2019**, *128*, 21−31.
(17) Smirnova, N. A.; Rakhman, I.; Moroz, N.; Basso, M.; Payappilly, J.; Kazakov, S.; Hernandez-Guzman, F.; Gaisina, I. N.; Kozikowski, A. P.; Ratan, R. R.; Gazaryan, I. G. *Chem. Biol.* **2010**, *17*, 380−391.
(18) Smirnova, N. A.; Osipyants, A. I.; Khristichenko, A. Y.; Hushpulian, D. M.; Nikulin, S. V.; Chubar, T. A.; Zakhariants, A. A.; Tishkov, V. I.; Gazaryan, I. G.; Poloznikov, A. A. *Russ. Chem. Bull.* **2018**, *67*, 150−156.
(19) Ahn, D.-R.; Kim, S. Y.; Lee, M. J.; Yang, E. G. *Bioorg. Med. Chem. Lett.* **2009**, *19*, 4403−4405.
(20) Frost, J.; Galdeano, C.; Soares, P.; Gadd, M. S.; Grzes, K. M.; Ellis, L.; Epemolu, O.; Shimamura, S.; Bantscheff, M.; Grandi, P.; Read, K. D.; Cantrell, D. A.; Rocha, S.; Ciulli, A. *Nat. Commun.* **2016**, *7*, 13312.
(21) Youssef, S.; Ren, W.; Ai, H.-w. *ACS Chem. Biol.* **2016**, *11*, 2492−2498.
(22) Kim, S. H.; Hwang, D.; Park, H.; Yang, E. G.; Chung, H. S.; Kim, S. Y. *Exp. Cell Res.* **2015**, *336*, 329−337.
(23) Konietzny, R.; König, A.; Wotzlaw, C.; Bernadini, A.; Berchner-Pfannschmidt, U.; Fandrey, J. *Ann. N.Y. Acad. Sci.* **2009**, *1177*, 74−81.
(24) Lee, K.; Zhang, H.; Qian, D. Z.; Rey, S.; Liu, J. O.; Semenza, G. L. *Proc. Natl. Acad. Sci. U.S.A.* **2009**, *106*, 17910−17915.
(25) Choi, C. Y.; Paulmurugan, R.; Ghambir, S.; Koong, A. C.; Le, Q. T.; Giaccia, A. J. *Int. J. Radiat. Oncol., Biol., Phys.* **2005**, *63*, S133−S134.
(26) Dixon, A. S.; Schwinn, M. K.; Hall, M. P.; Zimmerman, K.; Otto, P.; Lubben, T. H.; Butler, B. L.; Binkowski, B. F.; Machleidt, T.; Kirkland, T. A.; Wood, M. G.; Eggers, C. T.; Encell, L. P.; Wood, K. V. *ACS Chem. Biol.* **2016**, *11*, 400−408.
(27) Kim, S.; Yang, E. *Molecules* **2015**, *20*, 20551−20568.
(28) Cannaert, A.; Vandeputte, M.; Wille, S. M. R.; Stove, C. P. *Crit. Rev. Toxicol.* **2019**, *49*, 95−109.
(29) Wouters, E.; Walraed, J.; Banister, S. D.; Stove, C. P. *Biochem. Pharmacol.* **2019**, *169*, 113623.
(30) Haase, V. H. *Exp. Cell Res.* **2017**, *356*, 160−165.
(31) Miranda, E.; Nordgren, I. K.; Male, A. L.; Lawrence, C. E.; Hoakwie, F.; Cuda, F.; Court, W.; Fox, K. R.; Townsend, P. A.; Packham, G. K.; Eccles, S. A.; Tavassoli, A. *J. Am. Chem. Soc.* **2013**, *135*, 10418−10425.
(32) Raval, R. R.; Lau, K. W.; Tran, M. G. B.; Sowter, H. M.; Mandriota, S. J.; Li, J.-L.; Pugh, C. W.; Maxwell, P. H.; Harris, A. L.; Ratcliffe, P. J. *Mol. Cell. Biol.* **2005**, *25*, 5675−5686.

https://doi.org/10.1021/acs.analchem.1c02923
Anal. Chem. 2021, 93, 14462−14470